J. Membrane Biol. 34, 39–54 (1977)

Intercellular Communication and Tissue Growth: IX. Junctional Membrane Structure of Hybrids between Communication-Competent and Communication-Incompetent Cells

W.J. Larsen*, R. Azarnia, and W.R. Loewenstein

Department of Physiology and Biophysics, University of Miami School of Medicine, Miami, Florida 33152

Received 25 October 1976

Summary. The structure of the membrane junctions of the hybrid cell system, examined in the companion paper in respect to competence for communication through cell-to-cell membrane channels, is here examined by freeze-fracture electron microscopy. The junctions of the channel-competent parent cell and of the channel-competent hybrid cells present aggregates of intramembranous particles typical of "gap junction"; those of the channel-incompetent parent cell and channel-incompetent segregant hybrid cells do not. Competence for junctional communication and for gap junction formation are genetically related. The junctions of the intermediate hybrid cells with incomplete channel-competence (characterized by cell-to-cell transfer of small inorganic ions but not of fluorescein), present special intramembranous fibrillar structures instead of discrete gap-junctional particles. The possibility that these structures may constitute coupling elements with subnormal permeability is discussed in terms of incomplete dominance of the genetic determinants of gap junction.

The preceding paper in this series described the permeability properties of the cell junctions of hybrids between a cell competent to communicate by junctional membrane channels and a cell incompetent to do so (Azarnia & Loewenstein, 1977). The present paper describes the structure of the junctions of some of these hybrid cells, as seen in freeze-fracture electron microscopy. We focus here on junctional membrane specializations, particularly on intramembranous particle aggregates of the gap-junction type (Goodenough & Revel, 1970; Chalcroft & Bullivant, 1970; McNutt & Weinstein, 1970, 1973; Revel, Yee & Hudspeth, 1971; Staehelin, 1972; Peracchia, 1973; Peracchia & Fernandez-Jaimovich, 1975; Gilula, 1974), which are widely thought to contain the membrane channels for cell-to-cell communication. This study complements our earlier work using transmission electron microscopy (Azarnia, Larsen & Loewenstein, 1974).

* *Present address:* Department of Anatomy, University of Iowa, Iowa City, Iowa 52242.

Materials and Methods

Cell material

The following cell types were used: human parent cell, mouse parent cell, hybrid cell clones *1a, 1b, 2bps, 3D, $1a_3$ps, 2dp, 9K, $1b_1$p, $1a_3$pk*. The origins of the two parent cell lines and the lineages of the hybrid clones are given in the companion paper (Azarnia & Loewenstein, 1977). The cells were from the same lines or clones as those used for the foregoing electrophysiological work.

Electronmicroscopy

Thin sectioning. The cells were fixed in the culture dishes for 30 min at room temperature with a solution containing 2.45% glutaraldehyde (Ladd Research Industries Inc.), 2% sucrose and 0.05 M cacodylate (pH 7.4). After rinsing, the cells were fixed in a solution of 1% osmium tetroxide and 0.05 M cacodylate, dehydrated, embedded in araldite and sectioned. The sections were stained with uranyl acetate and lead citrate, and viewed in a Phillips-300 electron microscope. Micrographs were taken at a magnification of 1,300–1,800× with a 35 mm camera, and printed at a final magnification of 6,000−12,000× for the determinations of cell surface density.

Freeze-fracture. The cells were fixed as for thin sectioning, but the fixation time was reduced to 5–15 min. The dishes were then placed on ice, and the cells infiltrated with glycerol (30%) for 3 hr. Subsequently, the cells were gently removed from the dishes with the aid of a rubber policeman, mounted on Balzers specimen holders, and rapidly frozen in Freon 22 chilled in a bath of liquid nitrogen. The tissues were fractured in Balzers freeze-fracture device (BA #301, Balzers High Vacuum Corporation). Platinum-carbon replicas were mounted on 300-mesh grids, and micrographs were taken at a magnification of 19,600–112,900× with a Phillips-300 electron microscope.

The membrane fracture faces were scrutinized for the presence of junctional specializations through the binocular optical microscope (10×) of the electron microscope at a total magnification of 196,000×. Almost all of the membrane studied was of fracture face *P*; (Branton *et al.*, 1975); junctional structures are more easily detected in the replicas of this face.

Morphometry

Total membrane area scanned. The area of the membrane fracture faces scrutinized was measured on 6,500× micrographs with a polar planimeter (620015 Keuffel and Esser Co.). The sum of these areas for each cell type is the *total membrane area scanned (Sc)* listed in Table 2.

Cell membrane area. The total cell membrane area ($S_{i\mathrm{TOT}}$) was estimated in densely packed cell regions on the basis of the stereological relation

$$S_{i\mathrm{TOT}} = S_{Vi} \cdot V$$

where S_{Vi} is the membrane area in a unit test volume of the cell (the membrane surface density) and V, the total volume of the cell (*cf.* Weibel, Kistler & Scherle, 1966). S_{Vi} was determined by means of linear probes, namely a planar array of 100 parallel lines, each of a length equivalent to 1 μm, with 200 end points. S_{Vi} is here given by

$$S_{Vi} = \frac{2N_i}{L_T}$$

Table 1. Primary data for estimation of cell membrane area

Cell type	Clone	Mean cell volume[a] μm^3	Membrane surface density (S_{Vi}) μm^{-1}	Apposed membrane surface density μm^{-1}
Parental				
Human		1,150	2.24	
Mouse		524	0.64	0.202
Hybrid				
Channel-competent	1*a*	1,218	0.89	
	1*b*	1,289	0.84	
Intermediate	$1a_3pk$	1,150	0.64	
	$1b_1p$	1,150	0.47	
Channel-incompetent segregant	2*bps*	634	0.98	0.362
	3*D*	634	0.65	
	$1a_3ps$	1,150	0.90	0.412
	2*dp*			
	9*K*	756	0.94	

[a] Determined by laser beam absorbance-scatter.

where N_i is the number of intersections of the membrane (contour) with the array of probe lines placed at random on random thin sections (100–200 sections for each cell type cut at varying angle to the plane of the dishes), and L_T, the total probe length. Table 1 lists the mean values of S_{Vi} obtained.

The mean cell volume (V) was determined on cells in suspension by means of a laser cytograph, 6300 Bio-Physics, Inc. This instrument measures V as a function of the absorbance and scatter of collimated light by single cells in file. The volumes tabulated (Table 1) represent in each case the means of $5–10 \times 10^4$ cells. The absorbance-scatter peaks were sharp and reproducible, indicating that the suspended cells were nearly spherical.

In the case of the mouse parent cell and the hybrid clones *2bps* and *3D*, a rough estimate of the total cell membrane area was also made on the basis of mean cell diameters, assuming spherical cell shape. This yielded values of, respectively, 314, 401 and 380 μm^2, expectedly underestimating the actual areas of the cells in the culture dishes (*compare* with the areas obtained by stereology of sections of cells in culture, Table 2).

S_c/S_{iTOT}. The ratio between the integrated membrane areas scanned (S_c) and the membrane area of a cell, S_c/S_{iTOT}, served as index of the number of (equivalent) cell surfaces that were scanned for a given cell type.

Apposed membrane area. For the noncoupling mouse parent cell and revertant clones *2bps* and la_3ps which lacked obvious junctional differentiations, we determined the membrane areas where the adjacent cells are closely apposed. The apposed cell membrane area is defined as areas of P fracture face surrounded by areas of E fracture face. This area was determined with the same stereological method as the total cell membrane area. Table 1 lists the corresponding apposed membrane areas of a unit test volume of the cells (*the apposed membrane surface density*); and Table 2, the apposed membrane areas (mouse parent cell, clones *2bps*, and $1a_3ps$). It will be noted that the "apposed cell membrane

Table 2. Gap Junction Frequency in the Parent and Hybrid Cells

Cell type	Clone	Freeze fracture						Thin section[d]	
		Membrane area of cell (S_{iTOT}) μm^2	Total membrane area scanned (S_c) μm^2	S_c/S_{iTOT} Number of equivalent cell surfaces scanned[e]	Apposed membrane area of cell[a] μm^2	Gap junction frequency		Apposed membrane length scanned[b] μm	Gap junction transections frequency per 100 μm
						Per cell	Per 1,000 μm^2 membrane area		
Parental									
Human		2,576	7,597	2.9		10	3.9	825	4.4
Mouse		335	2,873	8.6(27.1)	106	0	0	5,369	0
Hybrids									
Channel-competent	1*a*	1,084						1,615	0.37
	1*b*	1,183	5,486	4.6		5.4	4.7		[c]
Intermediate	$1a_3pk$	736	5,448	7.4		0	0		
	$1b_1p$	541	9,438	17.4		0	0		
Channel-incompetent	2*bps*	621	2,573	4.1(11.2)	230	0	0	3,584	0
segregant	3*D*	412	5,912	14.3		0	0		
	$1a_3ps$	1,035	3,090	3.0(6.5)	474	0	0	3,210	0
	2*dp*	—	260	—		0	0	6,472	0
	9*K*	711	4,178	5.9		0	0		

[a] Area of *P* fracture face of plasma membrane surrounded by areas of *E* fracture face.
[b] Total plasma membrane length scanned where apposed membranes are $\leqq 80$ μm.
[c] Gap junctions were identified in this clone in thin section; only a short stretch of membrane apposition was scanned.
[d] Data from Azarnia, Larsen and Loewenstein, 1974. *Proc. Nat. Acad. Sci. USA* **71**:880.
[e] In parentheses, the values of the number of equivalent cell surfaces scanned, based on apposed membrane area instead of S_{iTOT}.

areas" as defined for the present purposes are not identical with those defined in our previous publication (Azarnia *et al.*, 1974) based on thin sections. Estimations of minimum S_c/S_{iTOT} for the mouse parent cell, clone *2bps*, and clone *1a*$_3$*ps* are given in Table 2.

Results

The Membrane Junctions

Table 2 summarizes the data of the occurrence of gap junction in the various cell types. The human parent cell and the early-generation hybrid cells (clones *1a* and *1b*) had gap junctions. These cells were shown to be fully channel-competent in the preceding paper; they transfer both small inorganic ions and fluorescein through their junctions (Azarnia & Loewenstein, 1977). Fracture face *P* of these cells showed the aggregates of intramembranous particles similar to gap junctions in other vertebrate cells (Goodenough & Revel, 1970; Chalcroft & Bullivant, 1970; McNutt & Weinstein, 1970). The incidence of gap junction was 10/cell in the human parent cell and 5.4/cell in the early-generation hybrids. The mouse parent cell and the segregant hybrid cells (*2bps, 3D, 1a*$_3$*ps, 2dp, 9K*), which are channel incompetent, showed no gap-junctional particle aggregates. The intermediate hybrids, which presented an intermediate modality of channel competence (they transfer small inorganic ions, but not detectably the 330-dalton molecule fluorescein), failed to show these aggregates, too. These clones presented, however, arrays of fibrils, a junctional structure found also in the early-generation hybrid cells, but not in the parent cells.

Structural details of the junctions of the various cell types follow below.

Junctions of the Channel-Competent Human Parent Cell

Several gap-junctional aggregates of intramembranous particles were often observed in the same region of fractured membrane (Fig. 1*a*). The particle aggregates varied in size. The particles themselves were approximately 8 nm in diameter and were usually packed in rectilinear or hexagonal arrays separated by particle-free aisles (Fig. 1*b*). In the junction shown in Fig. 1*b*, the small, smooth patches overlying some of the *P* face particles probably represent small areas of *E* fracture face. In some replicas, these patches were impressed with patterns identical to the arrangement of particle aggregates and particle-free aisles found on the *P* fracture face (Fig. 1*c*). In other replicas, the *E* fracture face revealed the closely packed arrays of pits typical of gap junctions in many other tissues (Fig. 1*d*).

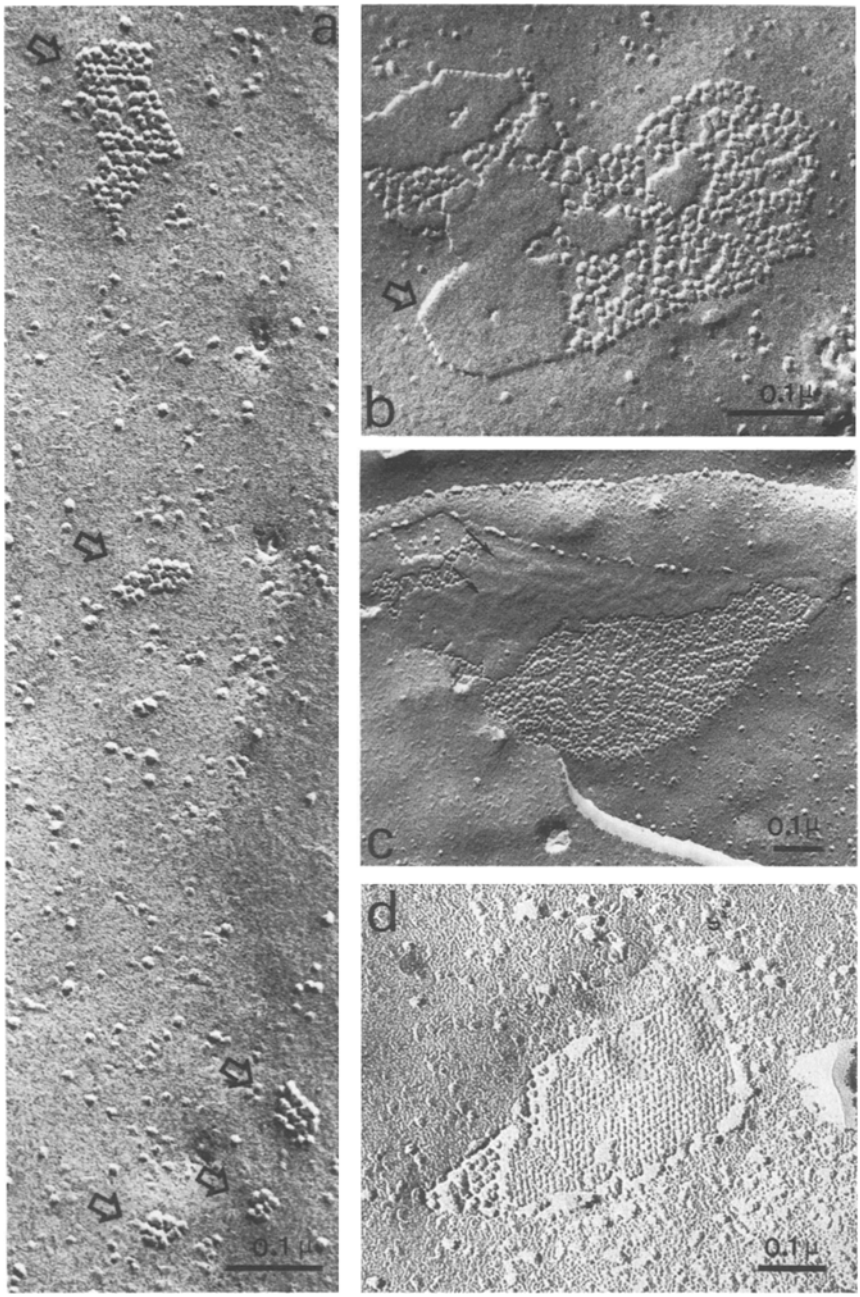

Fig. 1. Gap junctions in the human parent cell. (*a*) Replica of *A* fracture face. Several small aggregates of intramembranous particles are often found in close proximity (arrows). 132,200×. (*b*) Irregular gap junction. Small portions of the outer membrane leaflet of one cell (arrow) adhere closely to the membrane of the adjoining cell. 133,100×. (*c*) *E* fracture face (arrows) of this gap junction is impressed with a pattern similar to the arrangement of particles on the *P* fracture face. 63,500×. (*d*) Small pits in the *B* fracture face. 82,400×

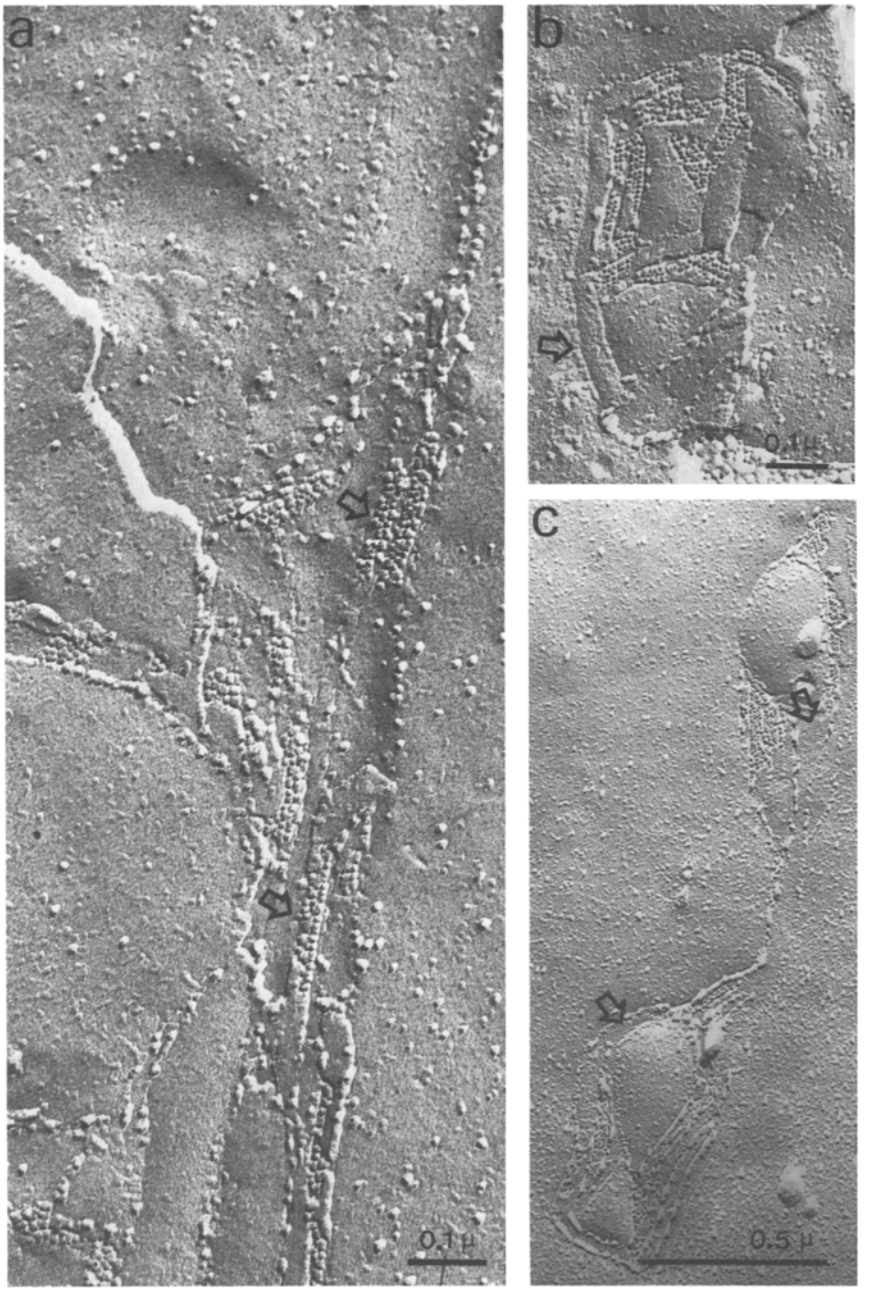

Fig. 2. (*a*) *P* fracture face particles in the human parent cell are occasionally organized in narrow rectilinear columns (arrows). 78,800×. (*b*) Narrow columns of *P* face particles are interspersed with small areas of nonjunctional membrane. Shallow *E* face groove borders one edge of this membrane specialization. 75,200×. (*c*) A junction similar to that of *b*, but with clearly visible pits in some areas of the *E* face (arrows). 50,100×

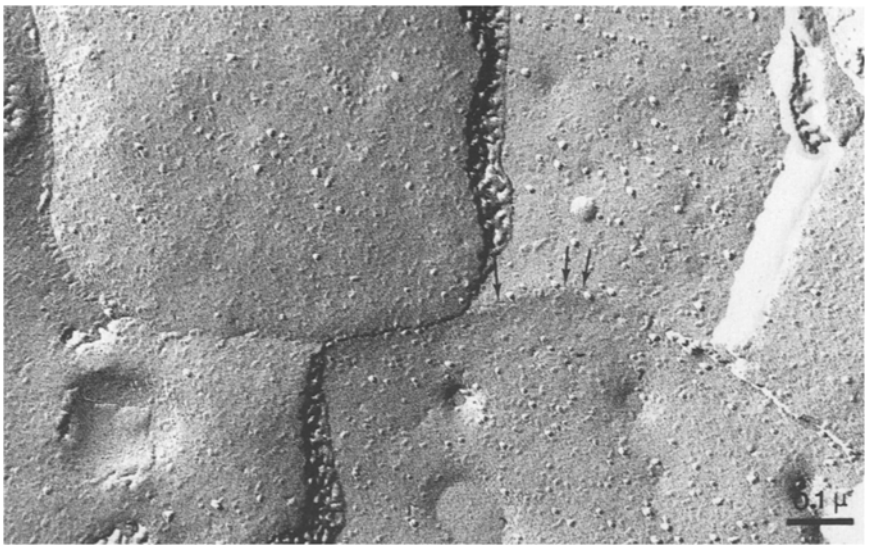

Fig. 3. *E* face groove and a narrow *P* face crack (human parent cell) are each continuous with a line of membrane fusion. 78,800

Occasionally the 8-nm particles were organized in rectilinear arrays, packed in columns separated from one another (Fig. 2*a*) or closely grouped together (Fig. 2*b*). These closely grouped columns were usually circumscribed by grooves containing irregular particles on the *E* fracture face (Fig. 2*c*). The adjacent membranes appeared to be fused in some replicas at the site of these grooves (Fig. 3). However, the grooves on the *E* fracture face are not identical with those seen in typical tight junctions of other tissues (Staehelin, 1972). In the replica of Fig. 3, it is obvious that the membranes of two neighboring cells come into intimate proximity or actually make contact along a line continuous with the groove in the *E* fracture face, and with a thin crack in the *P* fracture face. In other replicas, 10-nm particles were dispersed along these cracks and occasionally small aggregates of 8-nm particles were observed at one or at both ends (Fig. 4*a, b*) (*compare* with Yee & Revel, 1975). *E* face grooves were often associated with small areas of closely packed pits typical of gap junctions (Fig. 4*c, d*).

Junctions of the Channel-Competent Hybrid Cells

Small aggregates of 8-nm particles were observed on the *A* fracture face of membrane replicas of the channel-competent early-generation

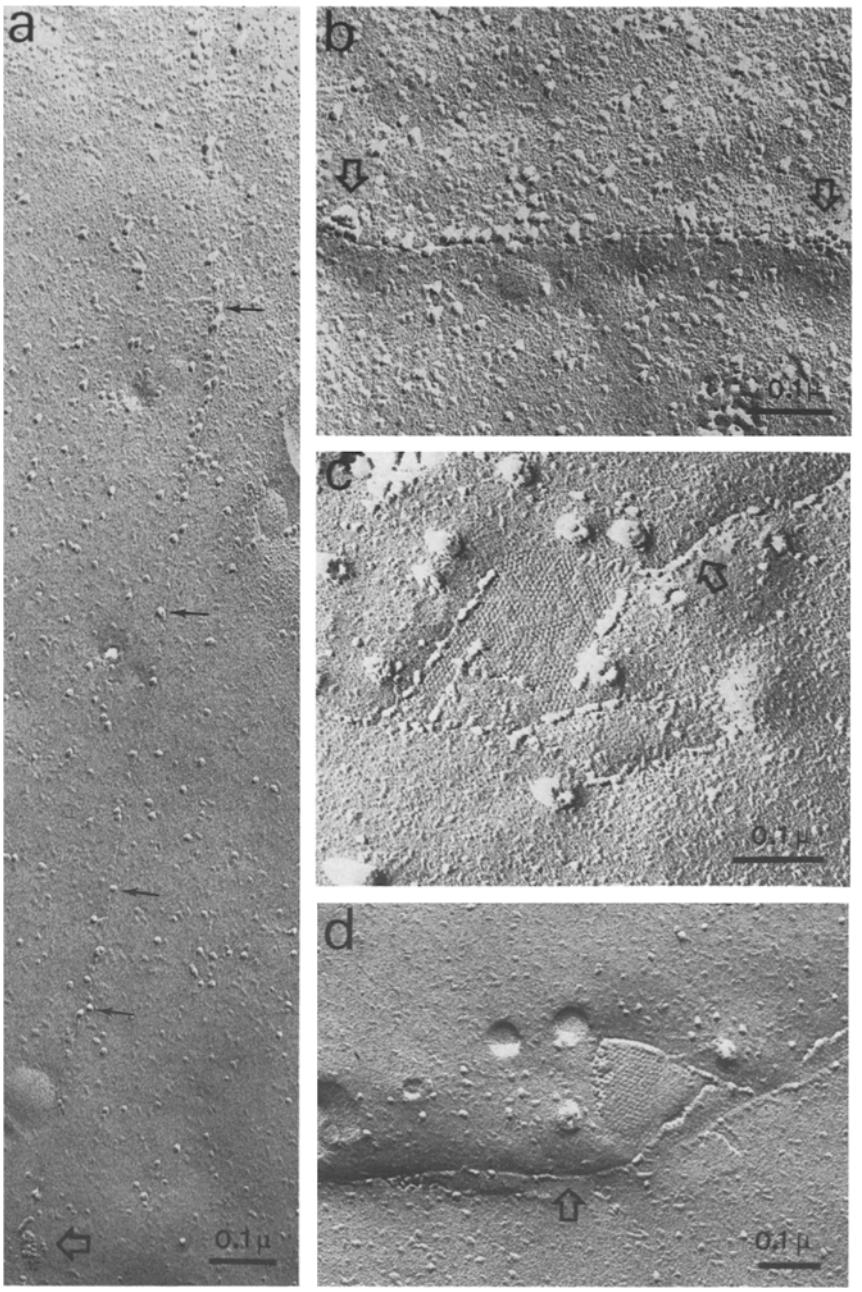

Fig. 4. (*a*) Human parent cell junction on a long, narrow *P* face crack with associated 10-nm particles (solid arrows) ends at a small aggregate of 8-nm particles (open arrow). 86,000×. (*b*) Short *P* face crack with 10-nm particles. Small aggregates of 8-nm particles are located at both ends (arrows). 113,800×. (*c*) *E* face grooves are often filled with irregular particles (arrow). 125,400×. (*d*) *E* face groove (arrow) continuous with a small gap junction. 78,800×

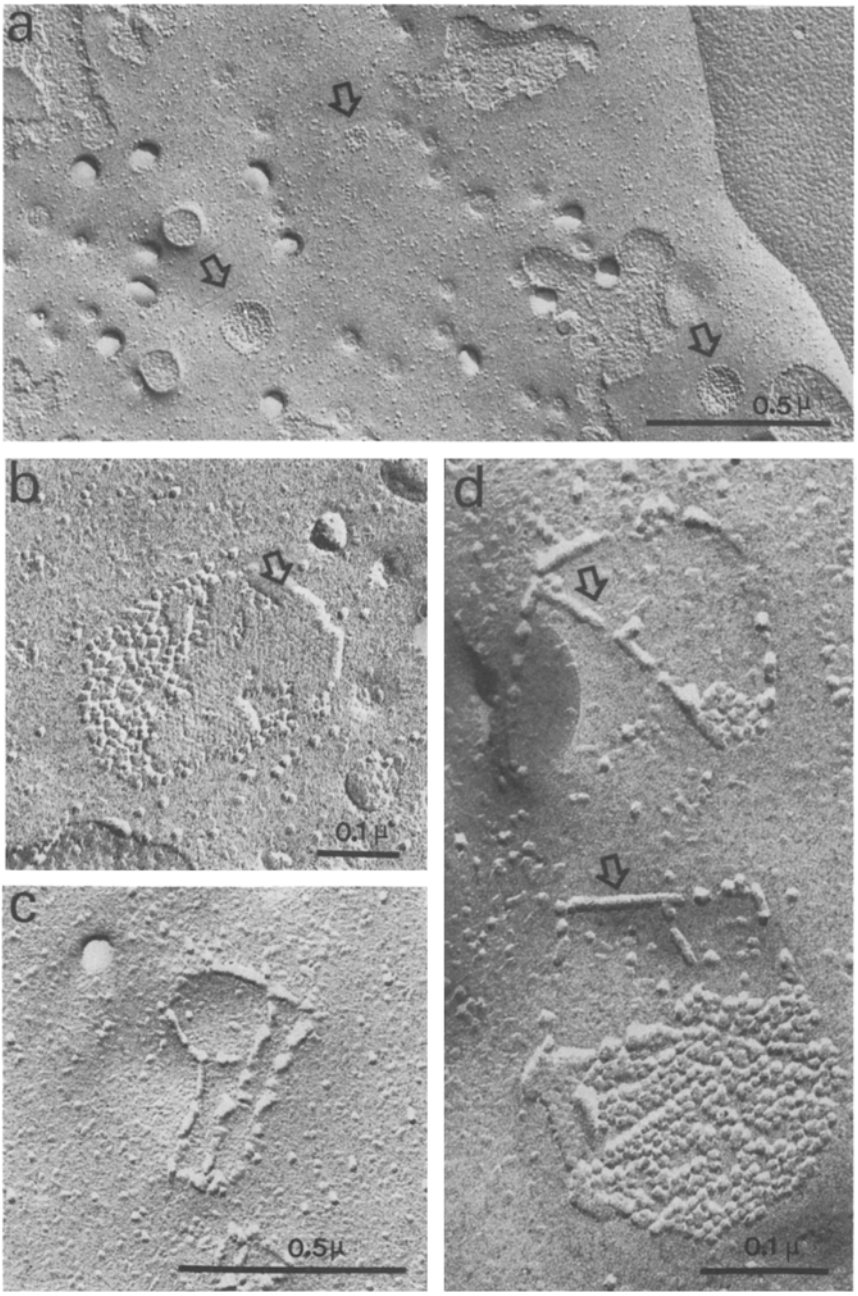

Fig. 5. Junctions of early-generation, channel-competent hybrid cells (clone *1b*). (*a*) Gap junctional particles on *P* fracture face (arrows). Small gap junctions are often found in the same region. 49,400×. (*b*) Pits in *E* fracture face. 103,800×. (c) Small array of fibrils on the *P* fracture face. 57,600×. (d) Occasionally *P*-face fibrils are associated with gap junctional particles. 118,200×

hybrid cell clones *1b*. Several aggregates were often present together on the same membrane (Fig. 5*a*). *E* fracture faces of some junctions showed closely packed pits (Fig. 5*b*). In this respect, the junctions were similar to those of the human parent cells.

In addition to the gap junction, small arrays of fibrils, of a diameter similar to that of the particles, were observed on the *P* fracture face. These structures occurred alone (Fig. 5*c*) or occasionally associated with gap-junctional particle aggregates (Fig. 5*d*). These fibrils were not seen in either parent cell line.

No *E*-face complements to the fibrils were obtained. For the reasons given in *Materials and Methods* the observations were mostly limited to *P* faces. The frequency of the fibrils was relatively low, and probably too low for us to find complementing grooves in the few observations on *E* faces.

Membrane Fracture Faces of the Intermediate Hybrid Cells

In the hybrid cell clones $1b_1pn$ and $1a_3pk$, with an intermediate expression of junctional communication, no gap-junction particle aggregates on *P* faces or tightly packed arrays of pits on *E* faces were observed. The total membrane area scanned was 9,438 μm^2 for clone $1b_1p$ and 5,448 μm^2 for clone $1a_3pk$, representing an equivalent surface area of 17.4 and 7.3 cells, respectively. However, these cells presented fibrillar arrays similar to those found on the *P* fracture faces of the early-generation hybrid cells (Fig. 5*c*), as well as a small number of *E* fracture face grooves (Fig. 4*d*).

Membrane Fracture Faces of the Channel-Incompetent Mouse Parent Cell and Segregant Hybrids

No gap junctions or tight junctions were observed in the channel-incompetent mouse parent cell line and channel incompetent segregant clones (*2bps, 3D,* $1a_3ps$*, 2dp, 9K*); intramembranous particles did not appear to be grouped in any obvious pattern. The total membrane areas scanned in each cell type and the equivalent number of cell surfaces scanned are listed in Table 2.

Observations on Hybrid Cell Size Related to Number of Chromosomes

For the purposes of the determinations of membrane area, we routinely measured the cell volumes of the various hybrid clones. The measurements were done on cells in suspensions (*see Materials and Methods*). A surprisingly simple relationship between cell volume and number of chromosomes thus became apparent (Table 3). The hybrid clones with the fewest chromosomes, the segregant clones *3D* and *2bps* (which had retained all or nearly all of the original mouse chromosome complement, but few chromosomes of the human complement; Table 2 of the preceding paper), had the smallest volumes, approaching that of the mouse parent cell. The hybrid clones with the largest number of chromosomes, the early-generation hybrid clones 1*a* and *1b* (descending from heterokarya with 1 human- and 2 mouse chromosome complements), had the largest volumes. Plotting the cell volumes against the modal number of chromosomes (which ranged 50 to 124), one gets the impression of proportionality (Fig. 6). Apparently, as in the giant polytene salivary gland cells of *Drosophila* and *Chironomus,* the cell volume of mammalian hybrid cells is related to the number of gene copies.

Table 3. Cell volume and number of chromosomes

Cell type	Hybrid clone	Number of chromosomes[a]	Cell volume μm^3
Parental			
Human		46 (0)	1150
Mouse		53 (1)	524
Hybrid			
Channel-competent	1*a*	104 (2)	1218
	1*b*	124 (2)	1289
Intermediate	$1a_3pk$	111 (2)	1150
	$1b_1p$	117 (2)	1150
Channel-incompetent segregant	2*bps*	49/59 (1)	634
	3*D*	54 (1)	634
	$1a_3ps$	102 (2)	1150
	9*K*	58 (1)	756

[a] Modal number; in parentheses, the number of mouse chromosome markers (*D*).

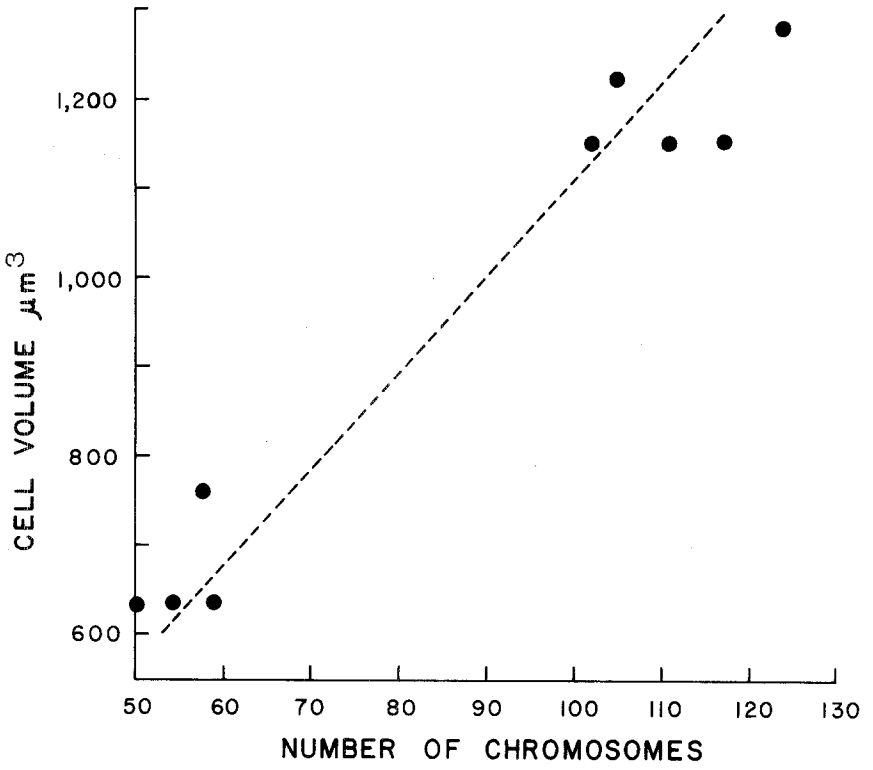

Fig. 6. Cell volume of the hybrid cells as a function of their number of chromosomes. *Ordinates:* the mean cell volume of each clone determined in cell suspension. *Abscissae:* the modal number of chromosomes of the clones. For clone *2bps,* which is bimodal, two values are plotted

Discussion

The present results show a genetic correlation between competence for junctional communication and competence for gap junction formation: the gap-junctional particle aggregates are present in the fully channel-competent human parent cells and early-generation hybrid cells, and are absent in the channel-incompetent mouse parent cells and segregant hybrid cells (Table 2). The factor of the human genome that corrects the gap-junction incompetence of the mouse parent in the hybrids seems identical with or linked to the factor that corrects the channel incompetence. Conclusive here is that, upon partial human chromosome loss, the hybrid cells, which show segregation in several other phenotypic traits (*see* preceding paper), resume both the gap-junction incompetence and the channel incompetence.

These results thus confirm our earlier work with transmission electron microscopy (Azarnia *et al.*, 1974). The present study is particularly satisfying, because the finding of gap-junctional absence in the channel-incompetent cells was obtained with a technique which offers broad scanning views of membrane, and which is capable of demonstrating gap junctional specialization most distinctly.

The *intermediate* hybrid clones (*$1b_1p$, $1a_3pk$*), which fall into a special class in regard to junctional communication, characterized by the capacity of cell-to-cell transfer of small inorganic ions (electrical coupling) but not of fluorescein, fall also into a special class in regard to junctional structure. These hybrid cells show no typical gap junctional particle aggregates, but they show a fibrillar junctional structure not present in either cell parent. The areas of membrane scanned in the two hybrid clones were 21–37 times greater than the mean membrane area containing one gap-junctional particle aggregate in the human parent cell. Hence, if such aggregates do at all occur in these hybrid cells, they are at least 21–37 times less abundant.

Thus, the question naturally arises of what constitutes the coupling structure in these intermediate hybrid cells. In terms of the notions that the gap-junctional particles contain the cell-to-cell channels and that these are normally permeable to both the small inorganic ions and fluorescein, two simple general answers suggest themselves: (i) the intermediate hybrid cells have relatively few gap-junctional particles; (ii) the pattern of aggregation of the particles in these cells is different from the general pattern. Alternative *i* rests on the point elaborated in the Appendix of the preceding paper that, when few channels are present, intercellular electrical coupling provides a more sensitive index of differences of channel abundance than fluorescein diffusion. Alternative *ii* would account for the electrophysiological results if the number of particles with functional channels in the deviant aggregates is reduced; or if the effective bore of the channels in these aggregates is reduced (*see* Dèlèze & Loewenstein, 1976; Rose, Simpson & Loewenstein, 1977; for examples of experimental reduction of the molecular size limits of channel permeation). Alternative *i* would be hard to verify with the electron microscopic methods presently at hand. The junctional particles mediating a detectable degree of electrical coupling may simply be too disperse or their aggregates too small for identification in freeze-fracture. Alternative *ii* merits a more detailed discussion in view of the finding of an exclusive hybrid junctional element, the fibrillar structure.

These fibrillar structures, in the early-generation hybrid clones, occur in occasional association with sizeable gap-junctional particle aggregates (Fig. 5*d*); in the intermediate hybrids, they occur alone. Thus, in terms of alternative *ii*, the possibility suggests itself that these fibrillar structures, which have about the same diameter as the gap-junctional particles, may be strings of such particles; that is, deviant particle aggregates of the above mentioned sort containing relatively few junctional channels or containing channels with reduced effective bore. Such deviations might conceivably be brought about by channel misalignment on the two membranes or by alterations in the channel structure itself. Viewed in this light, the fibrillar structures would be the structural equivalents of the expression of intermediacy of junctional communication described in the companion paper (Azarnia & Loewenstein, 1977).

The interesting genetic implication of this line of thought is that the gap-junction-competent character of the human parent cell is not completely dominant. This is not immediately apparent from the junctional phenotype of the early-generation hybrids. The incidence of gap junction in these channel-competent cells seems not very different from that in the human parent cell (Table 2); the expression of the corresponding gene(s) determining gap junction does not seem obviously impaired here by the presence of the mouse genome. However, such an impairment could become more overt in later-generations if, for example, one of the genes of a determinant pair is lost.

This then would entirely parallel the situation of the channel competence in these intermediate cells, and we may pattern an interpretation after that given in the companion paper for the electrophysiological results: the gap-junctional competence of the mouse parent cell, in principle, may be accounted for by a mutation in a structural or regulatory gene coding for a protein necessary for the assembly of the gap-junctional particle system. The lack of complete dominance of the human character thus may indicate that the defective protein product of the mouse gene enters into the hybrid gap-junctional assembly system, interfering with the normal assembly process. Depending on the proportion of normal and defective-proteins in the hybrid mixture, the cells would make fully channel-competent gap-junctional aggregates plus fibrillar aggregates with restricted channel competence (a combination seen in the early hybrids), or only the latter, fibrillar aggregates (as in the intermediate hybrids). The shift from one hybrid expression to the other may result from the loss of one of the two human chromosomes carrying the gene(s);

and the final switch to full junctional incompetence may result from loss of the whole chromosome pair.

This work was supported by research grant CA 14464 from the National Cancer Institute, National Institutes of Health.

References

Azarnia, R., Larsen, W., Loewenstein, W.R. 1974. The membrane junctions in communicating and non-communicating cells, their hybrids and segregants. *Proc. Nat. Acad. Sci. USA* **71**:880

Azarnia, R., Loewenstein, W.R. 1977. Intercellular communication and tissue growth. VIII. A genetic analysis of junctional communication and cancerous growth. *J. Membrane Biol.* **34**:1

Branton, D., Gilula, N.B., Karnovsky, M.V., Moore, H., Muhlentaler, K., Northcote, D.H., Packer, L., Jatir, B., Satir, P., Speth, V., Staehelin, L.A., Steare, R.L., Weinstein, R.S. 1975. Freeze-etching nomenclature. *Science* **190**:54

Chalcroft, J.P., Bullivant, S. 1970. An interpretation of liver cell membrane and junction structure based on observations of freeze-fractured replicas of both sides of the fracture. *J. Cell Biol.* **47**:49

Délèze, J., Loewenstein, W.R. 1976. Permeability of a cell junction during intracellular injection of divalent cations. *J. Membrane Biol.* **28**:71

Gilula, N.B. 1974. Junctions between cells. *In:* Cell Communication. R.P. Cox, editor. John Wiley, New York

Goodenough, D.A., Revel, J.P. 1970. A fine structural analysis of intercellular junctions in the mouse liver. *J. Cell Biol.* **45**:272

McNutt, N.S., Weinstein, R.S. 1970. The ultrastructure of the nexus, a correlated thin-section and freeze-cleave study. *J. Cell Biol.* **47**:666

McNutt, N.S., Weinstein, R.S. 1973. Membrane ultrastructure at mammalian intercellular junction. *Prog. Biophys. Mol. Biol.* **26**:45

Peracchia, C. 1973. Low resistance junctions in crayfish. II. Structural details and further evidence for intercellular channels by freeze-fracture and negative staining. *J. Cell Biol.* **57**:66

Peracchia, C., Fernandez-Jaimovich, M. 1975. Isolation of intramembrane particles from gap junctions. *J. Cell Biol.* **67**:330*a*

Revel, J.P., Karnovsky, M.J. 1967. Hexagonal array of subunits in intercellular junctions of the mouse heart and liver. *J. Cell Biol.* **33**:C7

Revel, J.P., Yee, A.G., Hudspeth, A.J. 1971. Gap junctions between electrotonically coupled cells. *Proc. Nat. Acad. Sci. USA* **68**:2924

Robertson, J.D. 1963. The occurrence of a subunit pattern in the unit membranes of club endings in Mauthner cell synapses in goldfish brains. *J. Cell Biol.* **19**:201

Rose, B., Simpson, I., Loewenstein, W.R. 1977. Calcium ion produces graded changes in permeability of membrane channels in cell junction. *Nature (London) (in press)*

Staehelin, L.A. 1972. Three types of gap junctions interconnecting intestinal epithelial cells visualized by freeze-etching. *Proc. Nat. Acad. Sci. USA* **69**:1318

Weibel, E.R., Kistler, G.S., Scherle, W.F. 1966. Practical stereological methods. *J. Cell Biol.* **30**:23

Yee, A.G., Revel, J.P. 1975. Endothelial cell junctions. *J. Cell Biol.* **66**:200